SIMULATION STUDY ON THE INFLUENCE OF TEMPERATURE-DEPENDENT ACOUSTIC-THERMAL PARAMETERS ON TISSUE LESION UNDER HIFU IRRADIATION

Hu DONG[1,2], Xiao ZOU[1], Shengyou QIAN[1]*

In this paper, the simulation is carried out by changing only the acoustic parameters and simultaneously changing the acoustic and thermal parameters, revealing the difference of influence of the acoustic and thermal parameters on tissue lesion and its variation law. With the increase of temperature corresponding to parameters, the predicted focal temperature and lesion area show a trend of decreasing first and then increasing. Moreover, predicted focal temperature and lesion area are underestimated by using acoustic parameters corresponding to T>61.5℃. Lesion area predicted by continuous high intensity focused ultrasound (HIFU) heating is larger than segment heating.

Keywords: high intensity focused ultrasound, focal temperature, temperature distribution, lesion.

1. Introduction

As an emerging modern method of tumor treatment, high intensity focused ultrasound (HIFU) can be focused into biological tissues which causes the energy of ultrasound to be locally absorbed in focal region at millimeter-level, and thus it will generate high temperature above 60 °C in focal position, resulting in thermal necrosis of biological tissues [1].The high temperature generated by HIFU cannot only kill tumor cells, but also directly ablate diseased tissues and denature proteins. The successful application of HIFU in clinical surgery is that it accurately transmits appropriate amount of thermal dose to treatment site [2,3]. Therefore, the understanding of temperature distribution information in biological tissues is a necessary prerequisite to ensure therapeutic effect of HIFU.

In most clinical or laboratory situations, it is difficult to accurately measure the internal temperature distribution in real time. Magnetic resonance imaging (MRI) can measure the temperature distribution of treatment area in a short time, and the dynamic temperature of treatment area can also be obtained by periodic continuous measurement, but this method is expensive and complex. The

[1] School of Physics and Electronics, Hunan Normal University, Changsha 410081, China
[2] School of Information Science and Engineering, Changsha Normal University, Changsha 410100, China, e-mail: wjd3203@163.com
∗Corresponding author, e-mail: shyqian@hunnu.edu.cn

Khokhlov-Zabolotskaya-Kuznetsov (KZK) and Pennes equations are often used in combination to predict temperature distribution and lesion area of biological tissues [4], but they need some acoustic parameters (such as sound velocity, density, nonlinear parameter B/A, attenuation coefficient) and thermal parameters (such as heat capacity coefficient, thermal conductivity coefficient) which related to biological tissues as a prior information for prediction, traditional methods usually use constant acoustic and thermal parameters at room temperature or body temperature for prediction [5-7].

Choi et al.[8] measured attenuation coefficient, sound velocity and B/A of ex-vivo porcine liver at different temperature by experiments. Guntur et al.[9] obtained the density, heat capacity coefficient and thermal conductivity coefficient of ex-vivo porcine liver at different temperature by experiments. The targeted physical properties of HIFU heating can effectively change internal temperature distribution of organism, i.e. the geometry of damage. Guntur et al.[10] theoretically studied the effect of temperature-related thermal parameters on heat distribution in ex-vivo porcine livers. Compared with the heat distribution predicted by thermal parameters corresponding to the temperature which cause thermal denaturation of biological tissues, the prediction of focal temperature and lesion area of porcine liver with constant thermal parameters at 25 ℃ was obviously overestimated. However, in actual HIFU treatment process, besides the change of thermal parameters with temperature of biological tissues, the acoustic parameters will also change with temperature of biological tissues. Therefore, it is particularly necessary to study the influence of temperature-related acoustic and thermal parameters on temperature distribution of biological tissues during HIFU treatment.

In this paper, the effects of temperature-related acoustic and thermal parameters on temperature distribution and lesion area of ex-vivo porcine liver under HIFU irradiation, as well as changes in acoustic and thermal parameters of porcine liver after heating were studied. The effects of segment heating and continuous heating on lesion area were analyzed. Acoustic and thermal parameters of ex-vivo porcine liver between 30 ℃ and 75 ℃ were used, KZK nonlinear acoustic equation was used to calculate HIFU sound field of porcine liver at different temperature, and Pennes bio-heat transfer equation was used to calculate temperature distribution and thermal lesion area of porcine liver with corresponding parameters.

2. Principles and methods

The KZK equation is used to establish the nonlinear sound field propagation model and perform sound field simulation. The KZK equation can be expressed as [11]

$$\frac{\partial^2 p}{\partial z \partial \tau} = \frac{c}{2}\nabla_{\perp}^2 p + \frac{\delta}{2c^3}\frac{\partial^3 p}{\partial \tau^3} + \frac{\beta}{2\rho c^3}\frac{\partial^2 p^2}{\partial \tau^2} \quad (1)$$

Among them, p, τ, c, ρ, δ, β and $\nabla_{\perp}$ are sound pressure, retarded time, sound velocity, density, acoustic conductivity of tissues, nonlinear coefficient of tissues and Laplace operator, respectively. $\tau = t - z/c$, $\nabla_{\perp}^2 = \frac{\partial^2}{\partial x^2} + \frac{\partial^2}{\partial y^2}$. When the sound frequency is f_0, the sound absorption coefficient of medium is α_0. Sound absorption coefficient of medium is generally equated with sound attenuation coefficient, and the relationship between attenuation coefficient and frequency is shown as follow [11]

$$\alpha(f) = \alpha_0 (f / f_0)^{\mu} \quad (2)$$

μ is the attenuation index and $\mu = 1.0 \sim 1.4$ [11]. In frequency domain, sound pressure can be expressed as Fourier series expansion [12]

$$p = \sum_{n=-\infty}^{\infty} C_n \exp(-in\omega\tau) \quad (3)$$

Where C_n is the complex coefficient of *nth* harmonic [13]

$$\frac{\partial C_n}{\partial z} = -\frac{in}{2} N \sum_{k=-\infty}^{\infty} C_k C_{n-k} - An^2 C_n + \frac{i}{4Gn}\Delta_{\perp} C_n \quad (4)$$

Among them, $N = \frac{F\omega\beta p_0}{\rho c^3}$, $A = \alpha F$, $G = \frac{\omega a^2}{2cF}$, p_0, F and a are initial surface acoustic pressure, geometric focal length and half-aperture of the transducer, respectively.

In the calculation of sound field, the sound intensity of HIFU transducer can be expressed by using the plane-wave approximation [14]

$$I = \frac{1}{2\rho c}\sum_{n=1}^{N} |\, p_n \,|^2 \quad (5)$$

Pennes bio-heat transfer equation is used to simulate focal temperature and lesion area, the bio-heat transfer equation can be expressed as [15]

$$\rho C_t \frac{\partial T}{\partial t} = k_t \nabla^2 T + Q_v \quad (6)$$

C_t is specific heat capacity, k_t is heat transfer coefficient of tissues, and T is temperature of tissues. The thermal relaxation time in biological tissues is based on the Cattaneo-Vemotte equation of non-Fourier heat conduction, and the thermal relaxation time is about 10^{-8}~10^{-12} s for homogeneous medium [16]. Pennes equation of biological heat transfer is based on the Fourier law of heat conduction. For simplicity, the Pennes equation assumes that biological tissues are

homogeneous and isotropic, and the effect of thermal relaxation time is ignored here [17]. It has been proved that Pennes equation is effective in analyzing the temperature distribution, especially the steady-state distribution in biological tissues [18-20]. The equation does not take into account heat loss caused by blood flow, and the heat accumulation caused by sound field can be expressed as [15]

$$Q_v = 2\alpha I \tag{7}$$

According to above heat accumulation formula, the heat generated by HIFU at the focal position is mainly determined by the attenuation coefficient of tissues and the sound intensity. The sound intensity is the strongest in the focal position while the sound intensity around the focus decreases rapidly, and this will cause the temperature of treatment area to rise rapidly to more than 65℃ in about 0.5~1 s, at the same time the temperature change of normal tissues around the target area is relatively small [21,22]. Because of the focusing effect of HIFU, it is not necessary to isolate normal tissues from the treatment area in actual treatment. Finite difference time domain method is used to solve the bio-heat transfer equation, and the distribution of temperature in biological tissues can be obtained. Though the high temperature induced by HIFU can kill the diseased cells, the lesion area cannot be determined only by temperature. The lesion of tissues is related to the denaturation of protein, which is related to thermal dose. The thermal dose depends on temperature and heat time, so high temperature does not necessarily lead to lesion and ablation of tissues. In other words, if the tissues temperature reach to a high level, but the heat time is too short, maybe no visible lesion will happen in tissues. The thermal dose is used to characterize the lesion state and it is equivalent to the heating time at 43 ℃. R=0.5 if T ≥43 ℃, and R=0.25 if T<43 ℃. Here, we use the equivalent thermal dose standard at 43 ℃ for 240 minutes as a threshold for lesion formation in biological tissues [23]. The lesion area of tissues will be calculated based on this thermal dose standard in next sections.

$$TD_{43℃} = \int_{t_0}^{t} R^{43-T(\tau)} d\tau \tag{8}$$

HIFU frequency of concave spherical transducer is f =1.0 MHz, the geometric focal length is F =7.9 cm, the half-aperture is a =2.5 cm, the sound power is P =50 W, and the duty cycle of HIFU sinusoidal pulse wave cluster is D =10%. The transmission distance of ultrasound in water is z_w =5 cm, and that in porcine liver is z_l =2.9 cm. Supposing the porcine liver is homogeneous medium, the thickness of porcine liver is L =5.2 cm, and the width is W =4 cm. The spatial grid parameters for simulation are dz =0.121 mm and dr =0.119 mm. The order of nonlinear harmonics is set 128, and the time step of sound field and temperature field is set dt =0.01 s.

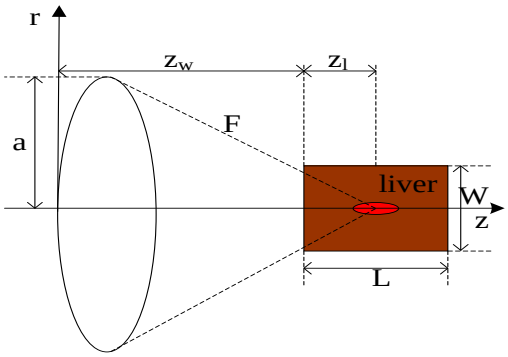

Fig. 1. Geometric configuration of high intensity focused ultrasound field radiation to liver

3. Acoustic and thermal parameters of liver at different temperature

Acoustic and thermal parameters of porcine liver are strongly correlated with temperature, and many experimental data have been obtained by relevant researchers. Choi and Guntur measured the attenuation coefficient, sound velocity, B/A, density, heat capacity coefficient and thermal conductivity coefficient of ex-vivo porcine liver [9,10]. Due to the short time of HIFU treatment, and this paper mainly studied temperature distribution of ex-vivo porcine liver under HIFU irradiation, so the influence of blood perfusion rate was neglected here. Combined with known acoustic and thermal parameters of porcine liver, following formulas are used to calculate temperature-related sound velocity, attenuation coefficient, density, B/A, heat capacity coefficient and thermal conductivity coefficient, and which are obtained by fitting with cftool toolbox of Matlab software [9,10].

$$\rho = 1084.09352 - 2.97434 \times T + 0.0042 \times T^2 + 0.00293 \times T^3 - 6.14447 \times 10^{-5} \times T^4 + 3.33019 \times 10^{-7} \times T^5 \quad (9)$$

$$c = 1529.3 + 1.6856 \times T + 6.1131 \times 10^{-2} \times T^2 - 2.2967 \times 10^{-3} \times T^3 + 2.2657 \times 10^{-5} \times T^4 - 7.1795 \times 10^{-8} \times T^5 \quad (10)$$

$$B/A = 6.68 - 0.41448 \times T + 0.03364 \times T^2 - 0.00101 \times T^3 + 1.34407 \times 10^{-5} \times T^4 - 6.35346 \times 10^{-8} \times T^5 \quad (11)$$

$$\alpha = 421 - 38.67 \times T + 1.85 \times T^2 - 0.04605 \times T^3 + 0.0005529 \times T^4 - 2.462 \times 10^{-6} \times T^5 \quad (12)$$

$$C = 3600 + 53.55552 \times T - 3.96009 \times T^2 + 0.10084 \times T^3 - 0.00106 \times T^4 + 4.01666 \times 10^{-6} \times T^5 \quad (13)$$

$$K = 0.84691 - 0.02094 \times T + 3.89971 \times 10^{-4} \times T^2 - 5.47451 \times 10^{-7} \times T^3 - 4.14455 \times 10^{-8} \times T^4 + 2.97188 \times 10^{-10} \times T^5 \quad (14)$$

The corresponding graph of above-mentioned fitted polynomial is shown in Fig. 2. The acoustic and thermal parameters corresponding to different temperature are calculated according to above formulas.

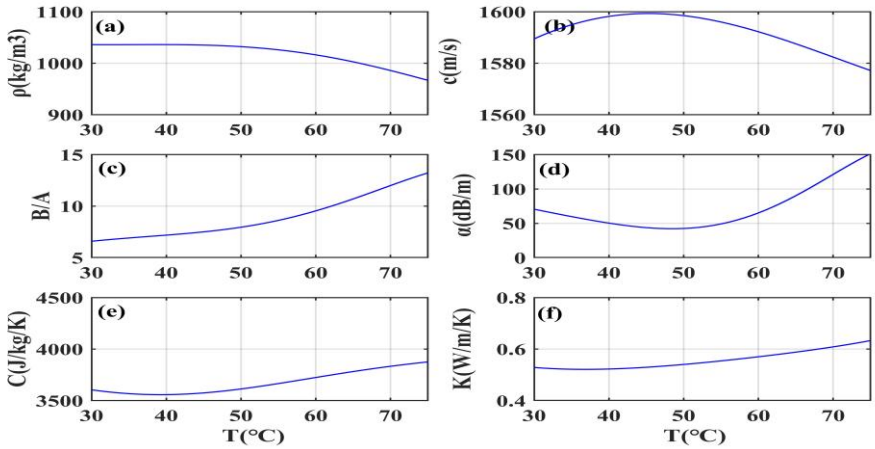

Fig. 2. Changes of acoustic and thermal parameters of porcine liver with temperature:(a) density; (b) speed of sound; (c) B/A; (d) attenuation coefficient; (e) heat capacity coefficient;(f) thermal conductivity coefficient.

4. Simulation results

4.1 Effect of acoustic parameters at different temperature on lesion area of porcine liver

In order to study the effect of acoustic parameters of porcine liver on focal temperature and lesion area at different temperature, the thermal parameters of porcine liver and water are set to be constant. The corresponding thermal parameters of porcine liver and water at 30 ℃ are shown in Table 1.

Table 1

Constant thermal parameters of liver and water at 30℃(1MHz)

Material	C(J/kg/K)	K(W/m/K)
Liver	3604	0.53
Water	4180	0.60

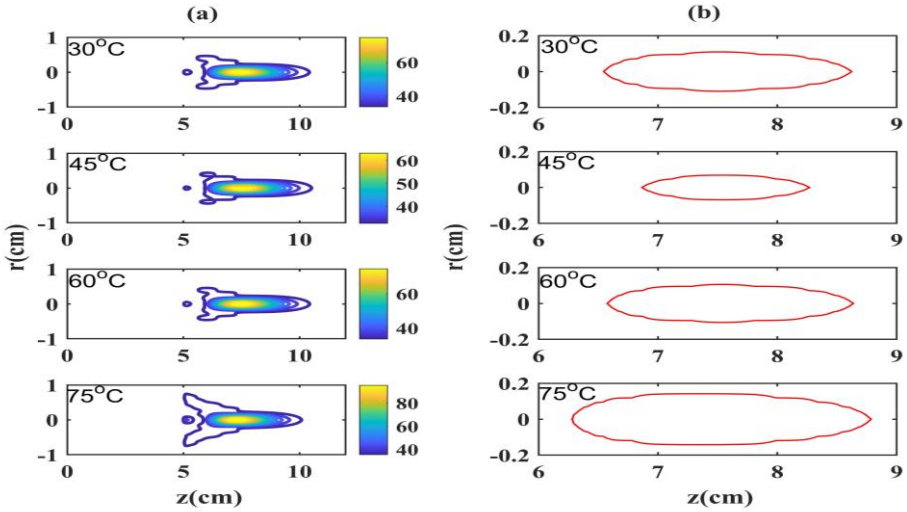

Fig. 3. Effect of acoustic parameters corresponding to different temperature on temperature distribution and lesion area with constant thermal parameters:(a) temperature distribution;(b) lesion area

From top to bottom, Fig. 3 (a) and Fig. 3 (b) show predicted temperature distribution and lesion area of ex-vivo porcine liver when thermal parameters are constant and acoustic parameters are corresponding to 30 ℃, 45 ℃, 60 ℃ and 75 ℃, respectively. The lesion area can be determined to use the thermal dose standard corresponding to the 240 minutes threshold proposed before, and it is measured with Photoshop software, which are 0.368 cm^2, 0.155 cm^2, 0.356 cm^2 and 0.605 cm^2, respectively. The lesion area predicted by corresponding acoustic parameters of porcine liver at 75 ℃ is the largest, while the lesion area predicted by corresponding acoustic parameters of porcine liver at 45 ℃ is the smallest. It shows that the lesion area predicted by the acoustic parameters corresponding to high temperature is larger and the tissues denaturation will be more obvious.

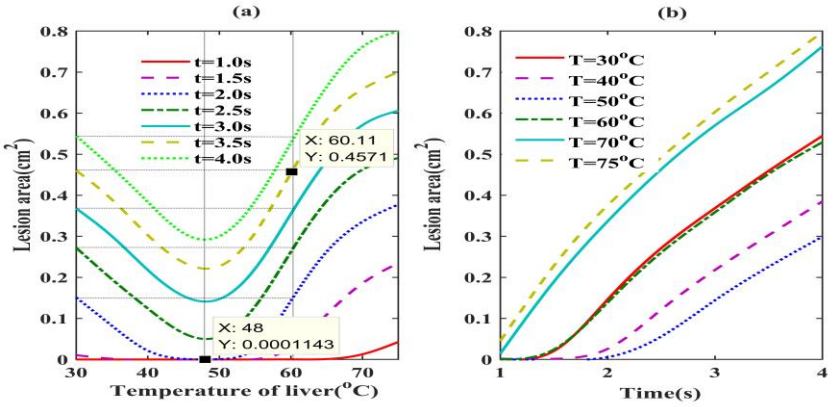

Fig. 4. The relationship between lesion area with constant thermal parameters and temperature corresponding to acoustic parameters and HIFU irradiation time:(a) lesion area predicted by acoustic parameters at different temperature;(b) effect of HIFU irradiation time on lesion area.

In Fig. 4 (a), although the irradiation time is different, the lesion area predicted by acoustic parameters corresponding to temperature from 30 ℃ to 75 ℃ of porcine liver decreases first and then increases with the increase of temperature corresponding to acoustic parameters. According to the distribution of thermal dose, the lesion area is predicted by acoustic parameters corresponding to T<60.11 ℃ of porcine liver is smaller than that predicted by acoustic parameters corresponding to T=30 ℃ of porcine liver. The lesion area predicted by acoustic parameters corresponding to T=48 ℃ is the smallest, while the lesion area predicted by acoustic parameters corresponding to T>60.11 ℃ of porcine liver is larger than that predicted by acoustic parameters corresponding to T=30 ℃ of porcine liver. In Fig. 2(d), it can be found that the attenuation coefficient decreases with the increase of temperature at 30 ℃≤T≤48 ℃, but it increases with the increase of temperature at 48 ℃<T≤75 ℃. The difference of attenuation coefficient corresponding to T=30 ℃ and T=60 ℃ of porcine liver is very small. When the irradiation time is t=1.0 s and t=1.5 s, respectively, and the acoustic parameters corresponding to 30 ℃<T<65 ℃ and 35 ℃<T<57 ℃ of porcine liver are used to predict lesion area, and the predicted results show that there is almost no lesion appear.

In Fig. 4 (b), the lesion area is predicted by acoustic parameters corresponding to different temperature of porcine liver, and it increases with the increase of irradiation time. Under the same condition of irradiation time, the predicted lesion area from large to small is corresponding to acoustic parameters of porcine liver at T=75 °C, 70 °C, 30 °C, 60 °C, 40 °C and 50 °C, respectively. In Fig. 2 (d), the value of attenuation coefficient from large to small is corresponding to the temperature of porcine liver at T=75 ℃, 70 ℃, 30 ℃, 60 ℃, 40 ℃ and 50 ℃, respectively. The predicted maximum and minimum lesion area are corresponding to the maximum and minimum attenuation coefficients of porcine liver, respectively.

4.2 Effects of acoustic and thermal parameters at different temperature on focal temperature and lesion area of porcine liver

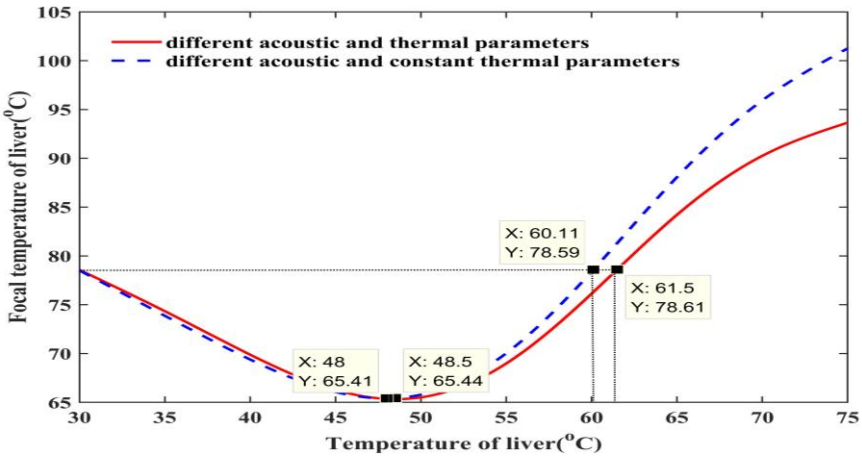

Fig. 5. Focal temperature predicted by acoustic parameters at different temperatures but thermal parameters at 30℃ and acoustic and thermal parameters at different temperature under 3s HIFU irradiation

In Fig. 5, HIFU irradiation time is 3 s, the focal temperature predicted by acoustic parameters, acoustic and thermal parameters of porcine liver from T=30 ℃ to T=75 ℃ decreases first and then increases. Among them, the focal temperature predicted by acoustic parameters of porcine liver corresponding to T=30 ℃ and T=60.11 ℃ is the same as that predicted by acoustic and thermal parameters of porcine liver corresponding to T=61.5 ℃. The focal temperature predicted by acoustic parameters of porcine liver corresponding to T=48 ℃ is the lowest, while the focal temperature predicted by acoustic and thermal parameters of porcine liver corresponding to T=48.5 ℃ is the lowest, the main reason for their difference is the influence of thermal diffusion. It can be found that the attenuation coefficient of porcine liver at T=48.5 ℃ is slightly larger than attenuation coefficients at T=48 ℃. Moreover, it can be found that the thermal conductivity coefficient of porcine liver at T=48.5 ℃ is also slightly larger than that at T=30 ℃ in Fig. 2 (f). Under the same condition of acoustic parameters, the difference of focal temperature predicted by acoustic parameters, acoustic and thermal parameters corresponding to temperature from T=30 ℃ to T=48 ℃ of porcine liver is very small. Fig. 2 (f) shows that thermal conductivity coefficient of porcine liver varies slightly from T=30 ℃ to T=48 ℃, and it indicates that acoustic parameters have a great influence at this moment, while the focal temperature predicted by acoustic parameters corresponding to temperature from T=48 ℃ to T=75 ℃ is higher than that predicted by acoustic and thermal parameters corresponding to the same temperature of porcine liver at the same time, and theirs difference of predicted focal temperature increases gradually. In Fig. 2 (f), it can be found that thermal conductivity coefficient of porcine liver

increases gradually from T=48 ℃ to T=75 ℃, which indicates that thermal parameters have a great influence at this moment.

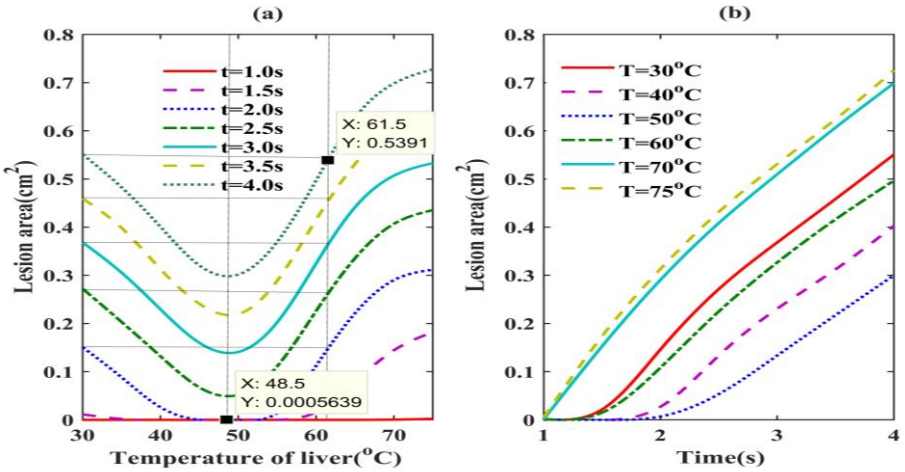

Fig. 6. The relationship between lesion area with simultaneous change of acoustic and thermal parameters and temperature corresponding to parameters and HIFU irradiation time:(a) lesion area predicted by acoustic and thermal parameters at different temperature;(b) effect of HIFU irradiation time on lesion area

In Fig. 6 (a), when the irradiation time is different, the lesion area predicted by acoustic and thermal parameters corresponding to the temperature of porcine liver between 30 ℃ and 75 ℃ decreases first and then increases with the increase of temperature corresponding to parameters. The lesion area is predicted by acoustic and thermal parameters corresponding to T<61.5 ℃ of porcine liver is smaller than that predicted by acoustic and thermal parameters corresponding to T=30 ℃ of porcine liver, which is related to the denaturation of tissues. The lesion area predicted by acoustic and thermal parameters is the smallest corresponding to T=48.5 ℃, while the lesion area predicted by acoustic and thermal parameters of porcine liver corresponding to T>61.5 ℃ is larger than that predicted by acoustic and thermal parameters of porcine liver corresponding to T=30 ℃. Similar to Fig. 4 (a), when the irradiation time is t=1.0 s and t=1.5 s, respectively, and the acoustic and thermal parameters corresponding to 30 ℃<T<75 ℃ and 34 ℃<T < 58 ℃ of porcine liver are used to predict lesion area, there is almost no lesion in porcine liver. In practical application, the irradiation time of HIFU should be selected according to the value of characteristic parameters of tissues. Compared with Fig. 4 (a), under the same irradiation time and parameters corresponding to same temperature, the lesion area is predicted by using the parameters corresponding to T>48 ℃ and it increases with temperature corresponding to the parameters, and the difference of predicted lesion area between Fig. 6 (a) and Fig. 4 (a) increases gradually. However, as the lesion area is predicted by using the

parameters corresponding to T<48 ℃, the difference of predicted lesion area between Fig. 6 (a) and Fig. 4 (a) is very small.

In Fig. 6 (b), the predicted lesion area increases with the increase of irradiation time by using acoustic and thermal parameters corresponding to different temperature of porcine liver. Under the same condition of irradiation time, the predicted lesion area from large to small is corresponding to the acoustic and thermal parameters of porcine liver at T=75 °C, 70 °C, 30 °C, 60 °C, 40 °C and 50 °C, respectively. When irradiation time is longer than 1.5 s, due to the influence of thermal diffusion, the lesion area predicted by acoustic and thermal parameters of porcine liver at T=30 ℃ and T=60 ℃ is significantly different in Fig. 6 (b).

4.3 Effect of segment heating and continuous heating on lesion area for porcine liver

Porcine liver at 30 ℃ is irradiated by HIFU for 2 s, and the lesion area is predicted by using the acoustic and thermal parameters corresponding to 30 ℃ of porcine liver. On this basis, porcine liver is irradiated for another 2 s, and the lesion area is predicted by using acoustic and thermal parameters corresponding to the temperature of porcine liver after first heating. In order to compare with the method of segment heating, porcine liver is irradiated at 30 ℃ with HIFU for 4 s at one time, and the lesion area is predicted by using acoustic and thermal parameters of porcine liver at 30 ℃. The simulation results show that the temperature of porcine liver after the first heating of segment heating is 66 ℃, and after the second heating is 72 ℃. The final temperature of one-time continuous heating reaches to 88 ℃. The lesion area predicted by segment heating and continuous heating is shown in Fig. 7 as below, and it can indicate the state of necrosis and ablation of biological tissues.

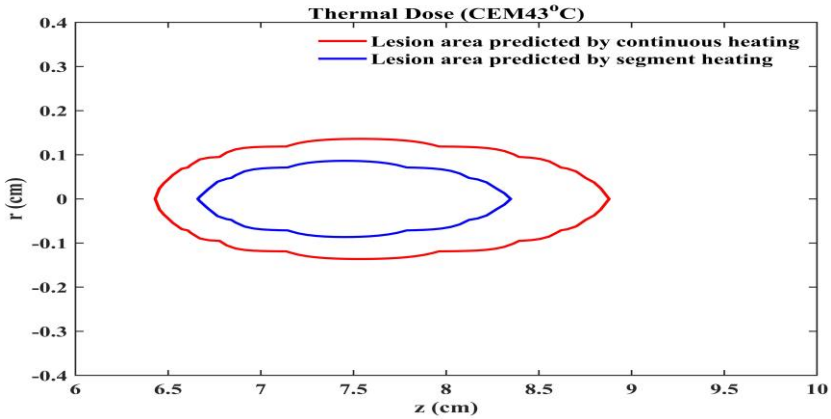

Fig. 7. Lesion area predicted by segment heating and continuous heating

In Fig. 7, the lesion area is firstly predicted by heating porcine liver from 30 ℃ for 2 s and then heating from 66 ℃ for another 2 s, and it is compared with

lesion area predicted by directly continuous heating from 30 ℃ for 4 s. The lesion area predicted by segment heating is obviously smaller than continuous heating.

5. Conclusion

Compared with traditional method of predicting temperature distribution in tissues by using constant acoustic and thermal parameters, the effects of acoustic and thermal parameters related to temperature of porcine liver on temperature distribution were studied. Under the same irradiation time, the focal temperature and lesion area predicted by acoustic parameters, acoustic and thermal parameters of porcine liver at different temperature decreases first and then increases with the increase of temperature corresponding to parameters. The focal temperature and lesion area predicted by acoustic and thermal parameters of porcine liver corresponding to 30 ℃ are smaller than those predicted by acoustic parameters, acoustic and thermal parameters corresponding to the temperature above 61.5 ℃. Because of thermal diffusion, under the premise of same temperature corresponding to acoustic parameters, when the temperature corresponding to parameters above 48 ℃, the focal temperature and lesion area predicted by changing acoustic and thermal parameters are smaller than that predicted by using thermal parameters corresponding to 30 ℃ and only changing acoustic parameters; when the temperature corresponding to parameters below 48 ℃, the differences of focal temperature and lesion area predicted between by changing acoustic and thermal parameters and only by changing acoustic parameters are all very small. By analyzing the influence of segment heating and continuous heating on lesion area, it can be found that lesion area induced by continuous heating is larger than segment heating. It can provide guidance for adjusting dosage of heating in HIFU operation and improve the safety of HIFU in clinical treatment.

Acknowledgments

This work was supported by the National Natural Science Foundation of China under grant No. 11774088,11474090, the Hunan Provincial Natural Science Foundation of China under grant No. 2018JJ3557, the Scientific Research Fund of Hunan Provincial Education Department under grant No. 17B025, and the Key Program of Changsha Normal University under grant No. 2019XJZK12.

R E F E R E N C E S

[1] *Li C, Yang Y, Guo X, Tu J, Huang P, Li Q, Zhang D*, Enhanced ultrasonic focusing and temperature elevation via a therapeutic ultrasonic transducer with sub-wavelength periodic structure, Appl. Phys. Lett., **vol.111**, no. 5, 2017, pp. 053701 (5 pages).

[2] *He M, Zhong Z, Li X, Gong X, Wang Z, Li F*, Effects of different hydrostatic pressure on lesions in ex vivo bovine livers induced by high intensity focused ultrasound, Ultrason. Sonochem., **vol.36**, 2017, pp. 36-41.
[3] *Hu J, Qian S, Ding Y*, Research on adaptive temperature control in sound field induced by self-focused concave spherical transducer, Ultrasonics, **vol.50**, no. 6, 2010, pp. 628-633.
[4] *Su H, Guo G, Ma Q, Tu J, Zhang D*, Noninvasive treatment efficacy monitoring and dose control for high-intensity focused ultrasound therapy using relative electrical impedance variation, Chin. Phys. B., **vol.26**, no. 5, 2017, pp. 243-252.
[5] *Nandlall S D, Jackson E, Coussios C C*, Real-time passive acoustic monitoring of HIFU-induced tissue damage, Ultrasound Med. Biol., **vol.37**, no. 6, 2011, pp. 922-934.
[6] *Ye G, Smith P P, Noble J A*, Model-based ultrasound temperature visualization during and following HIFU exposure, Ultrasound Med. Biol., **vol.36**, no. 2, 2010, pp. 234-249.
[7] *Ciubara A M, Dorohoi D, Severcan F, Creanga D*, Quantitative model of ultrasound propagation in biological media, U.P.B. Sci. Bull., Series A, **vol.76**, no. 4, 2014, pp. 221-226.
[8] *Choi M J, Guntur S R, Lee J M, Paeng D G, Lee K I, Coleman A*, Changes in ultrasonic properties of liver tissue in vitro during heating-cooling cycle concomitant with thermal coagulation, Ultrasound Med. Biol., **vol.37**, no. 12, 2011, pp. 2000-2012.
[9] *Guntur S R, Lee K I, Paeng D G, Andrew J C, Choi M J*, Temperature-dependent thermal properties of ex vivo liver undergoing thermal ablation, Ultrasound Med. Biol., **vol.3**9, no. 10, 2013, pp. 1771-1784.
[10] *Guntur S R, Choi M J*, Influence of temperature-dependent thermal parameters on temperature elevation of tissue exposed to high-intensity focused ultrasound: numerical simulation, Ultrasound Med. Biol., **vol.41**, no. 3, 2015, pp. 806-813.
[11] *Solovchuk M, Sheu T W H, Thiriet M*, Multiphysics modeling of liver tumor ablation by high intensity focused ultrasound, Commun. Comput. Phys., **vol.18**, no. 4, 2015, pp. 1050-1071.
[12] *Curra F P, Mourad P D, Khokhlova V A, Cleveland R O, Crum L A*, Numerical simulations of heating patterns and tissue temperature response due to high-intensity focused ultrasound, IEEE Trans. Ultrason. Ferroelectr. Freq. Control., **vol.47**, no. 4, 2014, pp. 1077-1089.
[13] *Li J L, Liu X Z, Zhang D, Gong X F*, Influence of ribs on the nonlinear sound field of therapeutic ultrasound, Ultrasound Med. Biol., **vol.33**, no. 9, 2007, pp. 1413-1420
[14] *Soneson J E*, A user-friendly software package for HIFU simulation, AIP Conference Proceedings, **vol.1113**, no. 1, 2009, pp. 165-169.
[15] *Chang S H, Cao R, Zhang Y B, Wang P G, Wu S J, Qian Y H, Jian X Q*, Treatable focal region modulated by double excitation signal superimposition to realize platform temperature distribution during transcranial brain tumor therapy with high-intensity focused ultrasound, Chin. Phys. B., **vol.27**, no. 7, 2018, pp. 078701 (10 pages).
[16] *Kaminski W*, Hyperbolic heat conduction equation for materials with a nonhomogeneous inner structure, ASME J. Heat Transfers, **vol.112**, 1990, pp. 555–560.
[17] *Liu J, Chen X, Xu L X*, New thermal wave aspects on burn evaluation of skin subjected to instantaneous heating, IEEE T. Bio-Med. Eng., **vol.46**, no. 4, 1999, pp. 420-428.
[18] *Bozkurt A, Roy R B, Ergün S*, Optimization of operating frequency of acoustic transducers for obtaining maximum temperature in HIFU based therapeutic ablation, IEEE Int Ultrasonics Symp., 2012, pp. 1-4.
[19] *Das K, Mishra S C*, Non-invasive estimation of size and location of a tumor in a human breast using a curve fitting technique, Int. Commun. Heat Mass, **vol.56**, 2014, pp. 63-70.
[20] *Huang H W*, Influence of blood vessel on the thermal lesion formation during radiofrequency ablation for liver tumors, Med. Phys., **vol.40**, no. 7, 2013, pp. 073303(13 pages).

[21] *Beerlage H P, van Leenders G J L H, Oosterhof G O N, Witjes J A, Ruijter E T, van de Kaa C A, Debruyne F M, de la Rosette J M C H*, High-intensity focused ultrasound (HIFU) followed after one to two weeks by radical retropubic prostatectomy: Results of a prospective study, Prostate, **vol.39**, no. 1, 1999, pp. 41-46.

[22] *Ter Haar G*, HIFU tissue ablation: concept and devices, Adv. Exp. Med. Biol., **vol.880**, 2016, pp. 3–20.

[23] *Sapareto S A, Dewey W C*, Thermal dose determination in cancer therapy, Int. J Radiat. Oncol., **vol.10**, no. 6, 1984, pp. 787-800.